Original Article

Spectral properties of the horizontal irradiance vertical distribution in Lake Teletskoye in August 2023: processing methodology and regional features

Suslin V.V.[1]*, Kudinov O.B.[1], Korchemkina E.N.[1], Latushkin A.A.[1], Sutorikhin I.A.[2], Kirillov V.V.[2], Martynov O.V.[1]

[1] FSBSI FRC Marine Hydrophysical Institute of RAS, Kapitanskaya str., 2, Sevastopol, 299011, Russia
[2] FSBSI Institute for Water and Environmental Problems, Siberian Branch of RAS, Molodezhnaya str., 1, Barnaul, Altai region, 656038, Russia

ABSTRACT. The sunlight spectral composition, penetrating to different depths in the upper water layer, on the one hand, depends on the optically active components contained in the water, on the other hand, it is important for the functioning of phytoplankton, and therefore plays an important role in the functioning of the aquatic ecosystem in general. When studying the spectral composition of light at different depths, a new instrument was used, made on a modern elemental basis. Analysis of the obtained spectra of the vertical attenuation coefficient made it possible to identify regional features of the penetration of natural sunlight characteristic of Lake Teletskoye.

Keywords: Lake Teletskoye, water optical properties, horizontal irradiance spectrum, PAR and horizontal irradiance profiles, light absorption coefficient, regional features

For citation: Suslin V.V., Kudinov O.B., Korchemkina E.N., Latushkin A.A., Sutorikhin I.A., Kirillov V.V., Martynov O.V. Spectral properties of the horizontal irradiance vertical distribution in Lake Teletskoye in August 2023: processing methodology and regional features // Limnology and Freshwater Biology. 2024. - № 5. - P. 1253-1266. DOI: 10.31951/2658-3518-2024-A-5-1253

1. Introduction

Sunlight penetrating into the water column is weakened by absorption and scattering by optically active substances (phytoplankton pigments, dissolved organic matter, suspended particles of various origins). The spectral variability of the optical properties of these components determines the resulting spectrum of underwater irradiance at different depths. The vertical distribution of irradiance is important for the phytoplankton functioning and, therefore, for the aquatic ecosystem as a whole. Estimation of the vertical distribution of underwater irradiance and the vertical attenuation coefficient of irradiance is required to model the photosynthesis processes of a specific reservoir. This is especially important for bounded water bodies, such as lakes, which are sensitive to both climate change and anthropogenic influence (Akulova et al., 2017; Aslamov et al., 2020; Churilova et al., 2020; Suslin et al., 2020).

In August 2023, comprehensive hydrooptical studies were performed on Lake Teletskoye, which included measurements of underwater irradiance spectra and the reflectance coefficient of the water column. Lake Teletskoye is located in the north-eastern part of the Altai Republic (Fig. 1a). It has an elongated shape and consists of two parts: a meridional part with a length of 50 km and a latitudinal (northern) one with a length of 28 km. Lake Teletskoye is a flowing lake, with more than 150 permanent rivers and temporary streams flowing into it, the largest of which is the Chulyshman River, which provides up to 70% of the total water inflow, and the Biya River flows out (Selegey et al., 2001).

Previous optical measurements on Lake Teletskoye were presented by spectra of underwater irradiance and light attenuation coefficient (Sutorikhin et al., 2020; Akulova et al., 2022). The aim of this work was to calculate the spectrum of the vertical light attenuation coefficient using spectral measurements of the horizontal irradiance profile, estimate the spectral slope of the total light absorption coefficient in the shortwave part of the spectrum and identify regional features characteristic of Lake Teletskoye. As an additional task, based on synchronous measurements of the photosynthetically active radiation (PAR) profile and the horizontal irradiance spectrum, to develop a method for constructing the attenuation profile of the horizontal irradiance spectrum in physical units.

*Corresponding author.
E-mail address: slava.suslin@mhi-ras.ru (V.V. Suslin)

Received: June 17, 2024; ***Accepted:*** October 02, 2024;
Available online: October 31, 2024

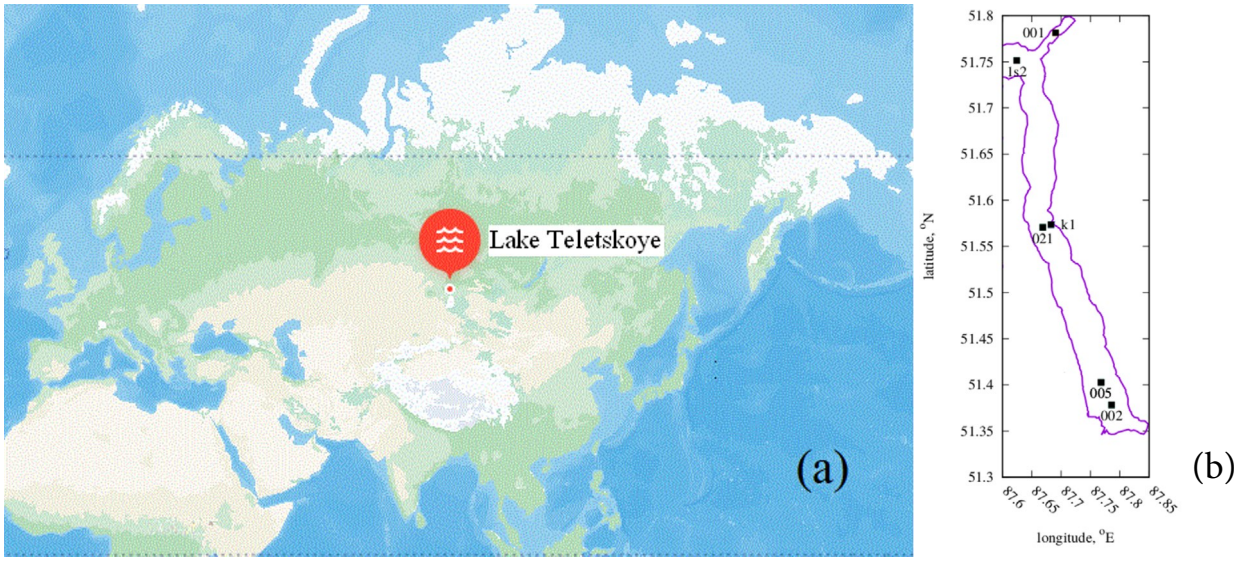

Fig.1. Geographical location of (a) Lake Teletskoye and (b) stations at which measurements of the spectral irradiance profile were carried out in August 2023.

2. Materials and methods

The stations positions at which synchronous spectral measurements of the horizontal irradiance profile and the PAR profile were carried out are shown in Fig. 1b. The figure shows that the measurements cover the northern, central and southern parts of the lake, including its estuary areas. Thus, we have representative station coverage of all major areas of the lake.

To study the light spectra at different depths, a new instrument made on a modern elemental basis was used (Latushkin and Kudinov, 2019). The instrument performed synchronous measurements of irradiance profiles in seven spectral bands with central wavelengths of 380, 443, 490, 510, 555, 590 and 620 nm. The bandwidth in the first spectral band is 30 nm, in all others – 10 nm. An example of measuring horizontal irradiance profiles in all seven spectral bands at the station 002 is shown in Fig. 2.

To solve one of the listed problems, measurements of the PAR profile were used with the "CONDOR" instrument (Lee, 2012; Hydrobiophysical multiparametric submersible autonomous complex "CONDOR". URL: https://dent-s.narod.ru/kondor.html), which were carried out synchronously with the measurement of horizontal irradiance. An example of measurements a PAR profile at station 002 by "CONDOR" instrument is shown in Fig. 3.

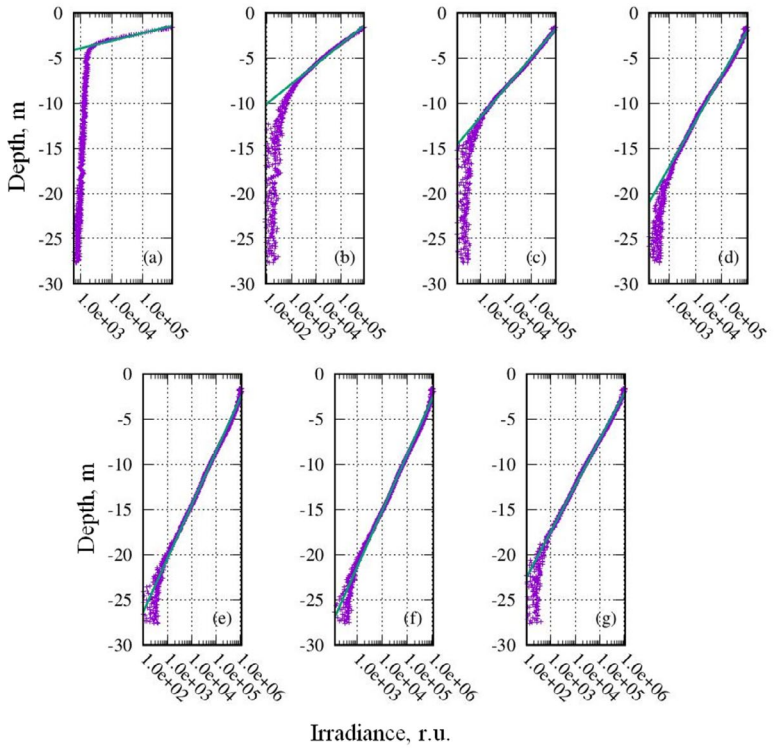

Fig.2. Example of measuring horizontal irradiance profiles at the station 002 in seven bands with a central wavelength: 380 nm (a), 443 nm (b), 490 nm (c), 510 nm (d), 555 nm (e), 590 nm (f) and 620 nm (g). Straight line is the result of approximation by Equation 4 for the corresponding band.

Let us describe a method for determining the integral value of photosynthetically active radiation immediately below the water surface using direct measurements of the *PAR*(*z*) profile, where *z* is the depth. From the definition of vertical attenuation coefficient (K_d) it follows that $PAR(z) = PAR \cdot \exp(-K_d \cdot z)$. After taking logarithms, the solution is reduced to finding the constants *a* and *b* in the linear equation (1):

$$y = a + b \cdot z, \quad (1)$$

where $a = \ln(PAR(0^-))$ and $b = -K_d$.

K_d was considered independent of *z* and was determined from *PAR*(*z*) measurements for an area just below the surface (*z* > 2–3 m) to avoid the influence of the ship's shadow. The measurements were carried out over several minutes to minimize errors associated with variable illumination of the water surface, such as cloudiness. Having determined the coefficient *a*, we find the photosynthetically active radiation immediately below the water surface $PAR(0^-)$. In Fig. 3 the blue dot shows an example calculation for station 002.

The method for calibrating horizontal irradiance measurement bands using synchronous measurements of the *PAR*(*z*) profile consists of three stages. For both instruments, we assumed that the following conditions were met: linearity of the scales and stability of the measuring scales during the expedition cycle.

2.1. Stage 1

We have initial telemetry measurements $O^T(\lambda_i, z)$, where λ_i is the central wavelength of the spectral band in nm, *i* is the number of the band from 1 to 7, *z* is the horizon depth in meters. Let's find the average value for each band for depths greater than 30 m $\left\langle O^T(\lambda_i, z > 30m)\right\rangle$ – dark signal. Note that $\left\langle O^T(\lambda_i, z > 30m)\right\rangle$ was determined for depths almost twice as large as the photosynthesis layer, i.e., at the lower boundary of which the radiance incident on the water surface in the range from 400 to 700 nm was attenuated 100 times

$$\left\langle O^T(\lambda_i, z > 30m)\right\rangle = \frac{1}{N} \cdot \sum_{z=30}^{z=z_{\max}} O^T(\lambda_i, z), \quad (2)$$

where *z* is the measurement depth, starting from 30m; z_{max} – maximum measurement depth for the corresponding station; *N* – number of measurements from 30m to z_{max}.

To test the hypothesis of the stability of the "dark" telemetric signal of horizontal irradiance for seven bands, measurements were used at the station 002 and 021. The time difference between measurements at these stations was 2 days. The results are presented in Fig. 4 and Table 1. Table 1 shows the average value of $\left\langle O^T(\lambda_i, z > 30m)\right\rangle$, their standard deviation (SD) and the number of measurements *N*. From Fig. 4 it is clear that the calibrations are stable.

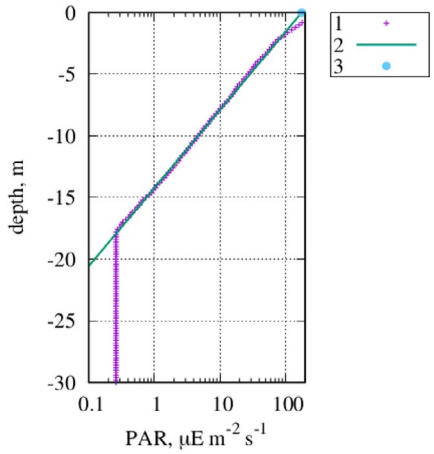

Fig.3. An example of measuring the PAR profile with the "CONDOR" instrument at station 002

1 – symbol "+";

2 – result of approximation of variation with depth by equation (1);

3 – $PAR(0^-)$ value, as a result of interpolation of equation (1) at 0 when z→0.

2.2. Stage 2

The calculation of the signal taking into account the dark current $O^u(\lambda_i, z)$ is performed according to the expression:

$$O^u(\lambda_i, z) = O^T(\lambda_i, z) - \left\langle O^T(\lambda_i, z > 30m)\right\rangle \quad (3)$$

where $\left\langle O^T(\lambda_i, z > 30m)\right\rangle$ – dark current values (see Table 1). Calculation of $a(\lambda_i)$ and $b(\lambda_i)$ was carried out for each station and for each of the seven bands according to the formula:

$$\ln(O^u(\lambda_i, z)) = b(\lambda_i) \cdot z + a(\lambda_i), \quad (4)$$

where the horizontal irradiance in the band with a central wavelength λ_i, immediately below the water surface was as $O^u(\lambda_i, 0^-) = \lim_{z \to 0^-}(O^u(\lambda_i, z))$ or $a(\lambda_i) = \ln(O^u(\lambda_i, 0^-))$, and the vertical light attenuation coefficient in the corresponding band λ_i as $K_d(\lambda_i, 0^-) = -b(\lambda_i)$. The results of calculations of coefficients $a(\lambda_i)$ and $b(\lambda_i)$ according to equation (4) for all seven stations are summarized in Table 2.

Table 1. Statistical characteristics of the "dark" telemetric signal of horizontal irradiance for seven bands at the station 002 and 021

Station number	$\left\langle O^T(\lambda_i, z > 30m)\right\rangle \pm$ SD							*N*
	380 nm	443 nm	490 nm	510 nm	555 nm	590 nm	620 nm	
002	16462 ± 91	12855 ± 90	12625 ± 112	15373 ± 99	19883 ± 88	14937 ± 101	14600 ± 95	333
021	16281 ± 90	12751 ± 79	12469 ± 98	15393 ± 96	19714 ± 103	14770 ± 98	14438 ± 97	88

2.3. Stage 3

The conversion of $O^p(\lambda_i, 0^-)$ into physical units of radiation was carried out using the expression:

$$O^p(\lambda_i, 0^-) = PAR(0^-) \cdot w_i, \quad (5)$$

where $w_i = \frac{1}{\Delta\lambda_i} \cdot \int_{\lambda_i - \Delta\lambda_i/2}^{\lambda_i + \Delta\lambda_i/2} w(\lambda) d\lambda$ is the fraction of photons in the corresponding spectral interval (Suslin et al., 2020), associated with the characteristics of the band $\lambda_i \pm \Delta\lambda_i/2$ (Lee, 2012); *PAR*(0-) – is found from measurements of the *PAR* profile using the "CONDOR" instrument. It is obvious that the form of $w(\lambda)$ depends on the altitude of the Sun and cloud conditions. In our case, the choice of the functional dependence of $w(\lambda)$ was taken from the work (Bartlett et al., 1998).

Then the conversion factor of telemetry into physical quantities is calculated using the formula

$$p(\lambda_i) = \frac{O^p(\lambda_i, 0^-)}{O^u(\lambda_i, 0^-)}. \quad (6)$$

Since we assumed that *PAR* is the integral of the number of photons lying in the spectral range from 400 to 700 nm, the band with a central wavelength of 380 nm was excluded from the calculation. The results of calculating $p(\lambda_i)$ are presented in Table 3.

3. Results and discussion

Figure 5 shows the K_d spectra and their difference from the average spectrum $\langle K_d \rangle$ for all seven stations (Table 2) after processing according to the method (equations (2) – (4)).

The minimum values of K_d in the band with a central wavelength of 590 nm, together with its high values in the spectrum short-wavelength region, indicate the dominance of absorption, primarily by the colored component of dissolved organic matter.

To identify the geographical features of K_d, consider Fig. 5b. Values of the difference $K_d - \langle K_d \rangle$ above average in the spectrum short-wave region are observed in the south of the lake (stations 002, 005 and 005*); minimum values – in the lake north of (stations 001 and 1s2); intermediate values in the center (st. k1 and 021). Thus, in the upper layer of the lake there is a tendency for water absorption to decrease from south to north (mainly related to the concentration of dissolved organic matter, since we are talking about a band with a central wavelength of 380 nm).

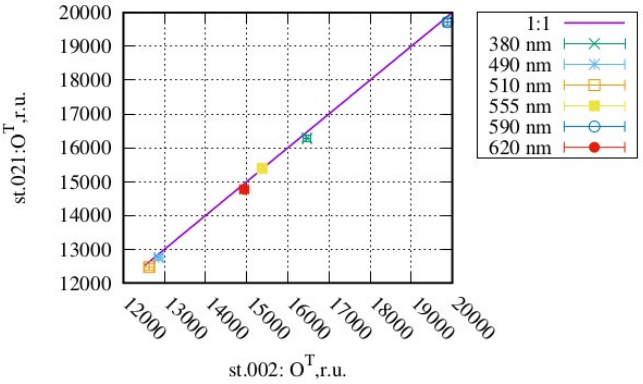

Fig.4. Test for the stability of calibrations during the expedition in seven bands using the example of station 002 and 021, separated by two days.

Let us note one more feature – the difference in K_d values in the band with a central wavelength of 443 nm at stations 001 and 1s2, located in the northern part of the lake. For station 001, located in Kamga Bay, this difference is significantly greater than at station. 1s2. This difference in K_d may be associated with additional absorption by phytoplankton, the concentration of which is significantly higher in the bay. However, this assumption requires additional verification.

The conclusion drawn from the analysis of Fig. 5a about the high value of the absorption coefficient by the upper layer of water in Lake Teletskoye is in good agreement with the results of measurements of the water reflectance spectra (R_{rs}) made by E.N.

Table 2. Results of calculations of coefficients $a(\lambda_i)$ and $b(\lambda_i)$ according to equation (4) for seven stations

Station	$a(\lambda_i)/b(\lambda_i)$						
	380	443	490	510	555	590	620
1 001	17.64 -2.733	15.17 -1.049	15.03 -0.705	14.67 -0.455	14.90 -0.393	14.80 -0.368	14.80 -0.453
2 002	19.15 -3.191	14.83 -1.116	14.23 -0.681	14.15 -0.483	14.32 -0.421	14.08 -0.400	14.00 -0.498
3 005	19.99 -3.491	16.27 -1.304	15.74 -0.815	15.32 -0.498	15.53 -0.465	15.29 -0.435	15.31 -0.559
4 005*	20.44 -3.211	16.48 -1.210	15.49 -0.703	14.99 -0.439	15.13 -0.386	14.99 -0.356	15.01 -0.458
5 021	17.90 -3.145	13.83 -1.023	13.42 -0.635	13.19 -0.438	13.29 -0.389	12.93 -0.361	12.96 -0.434
6 k1	19.87 -3.006	16.04 -0.966	15.95 -0.670	15.69 -0.473	15.80 -0.417	15.71 -0.398	15.79 -0.481
7 1s2	18.12 -2.789	15.01 -0.786	16.24 -0.655	16.38 -0.478	16.70 -0.431	16.38 -0.405	15.87 -0.451

* station 005 was performed with a time difference of 1 hour (3 – 13:00; 4 – 14:00 local time).

Table 3. The result of calculating $p(\lambda_i)$ in bands with a central wavelength λ_i and $O^p(\lambda_i, 0^-)$ for station k1

λ_i, nm	443	490	510	555	590	620
$p(\lambda_i)$	1.424e-06	1.967e-06	2.751e-06	2.731e-06	3.149e-06	2.978e-06
$O^p(\lambda_i, 0^-)$	1.321e+01	1.664e+01	1.786e+01	1.985e+01	2.098e+01	2.140e+01

Korchemkina during this expedition (Sutorikhin et al., 2020). A reference to the description of the instrument and method for the water column R_{rs} measuring is given in work (Shybanov et al., 2023). It is known that the absorption coefficient by dissolved organic matter in the Black Sea is significantly higher compared to the waters of the open ocean (Suetin et al., 2002; Kopelevich et al., 2004). Figure 6 shows examples of R_{rs} spectra of the water column in the Black Sea in April 2021 and in Lake Teletskoye at station 002 and 021 in August 2023. Note that the measurements in the Black Sea were carried out in the absence of coccolithophorid blooms. It is clearly seen that the value of the R_{rs} of the water column at a wavelength of 400 nm in Lake Teletskoye is more than three times less than in the Black Sea, despite the fact that in the long-wave region of the spectrum (more than 600 nm) the R_{rs} of the water column in the lake is greater than in the sea. On the one hand, this confirms the conclusion that the light absorption coefficient in the short-wave part of the spectrum in the lake is significantly higher than in the Black Sea. On the other hand, it is obvious that the light backscattering coefficient by suspended particles is significantly higher in the lake than in the sea. This is especially noticeable for station 002, located in the south at the confluence of the river Chulyshman, which carries a significant amount of suspended matter.

The obtained data on $K_d(\lambda)$ (Table 2) can be used to assess the spectral dependence S_{CDOM} of dissolved organic matter coefficient (a_{CDOM}), assuming that it makes the main contribution to the total absorption (atot) in the short-wavelength region of the spectrum ($\lambda \in 350 - 450$ nm), i.e. $a_{CDOM} >> a_w$, a_{ph}, $a_{tot} >> b_b$, and additionally $a_{tot} >> b_b$, where a_w and a_{ph} are the light absorption coefficients by pure water and phytoplankton, b_b is the total light backscattering coefficient by water, then:

$$K_d(\lambda) \approx const \cdot (a_{tot}(\lambda) + b_b(\lambda)) \approx const \cdot (a_w(\lambda) + a_{ph}(\lambda) + a_{CDOM}(\lambda) + b_b(\lambda)) \approx const \cdot a_{CDOM}(\lambda) . \quad (7)$$

Taking into account that the functional relationship a_{CDOM} from λ has the form (Kopelevich, 1983):

$$a_{CDOM}(\lambda) = a_{CDOM}(\lambda_0) \cdot \exp(-S_{CDOM} \cdot (\lambda - \lambda_0)), \quad (8)$$

and, having made elementary transformations of equation (7), taking into account equation (8) for two bands with a central wavelength $\lambda = 380$ nm and $\lambda_0 = 443$ nm, respectively, we obtain the expression for S_{CDOM}:

$$S_{CDOM} = \frac{1}{\lambda - \lambda_0} \cdot \ln\left(\frac{K_d(\lambda_0)}{K_d(\lambda)}\right). \quad (9)$$

The calculation results are presented in Table 4.

Presented in Table 4 results coincided with studies of the primary hydrooptical characteristics of Lake Teletskoye carried out a year earlier at the same time (Moiseeva et al., 2023), during which they directly measured the spectral variation of the colored component of dissolved organic matter for a similar stations grid and which showed that the variability of S_{CDOM} lies in the range of 0.017 – 0.019 nm^{-1} in the wavelength range 350 - 500 nm.

Figure 7 shows an example of recovering the spectrum of horizontal irradiance in physical units, obtained using the method described above (equations (2) – (6)) from measurements at k1 station. The behavior of the irradiance spectrum with depth (a sharp fail in the short-wavelength region of the spectrum) indicates a high content of dissolved organic matter in the Lake Teletskoye waters (Fig. 7). Features in the short-wave region of the horizontal irradiance spectrum and its maximum, starting from 5 m depth and below, correspond to a wavelength of 590 nm, also coincides with the results obtained a year earlier by employees of the Institute of Biology of the Southern Seas of RAS (Churilova et al., 2023).

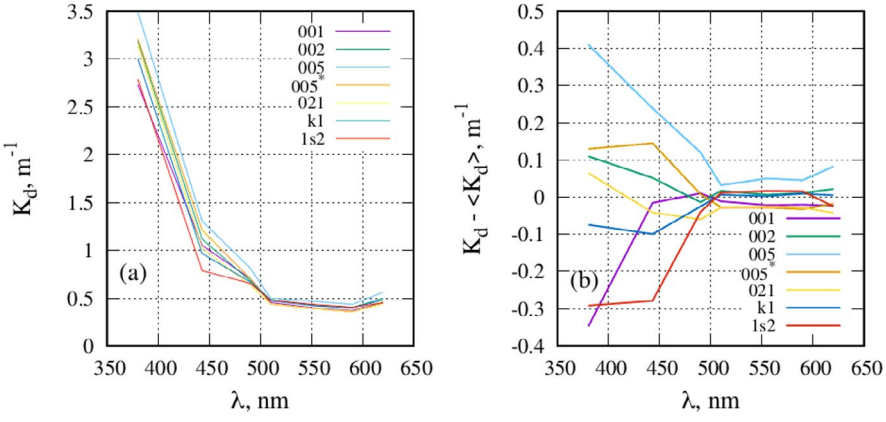

Fig.5. Spectra of the vertical light attenuation coefficient K_d (a) and their deviations from the average ($K_d - \langle K_d \rangle$), (b) for the sample (Table 2).

Table 4. Results of calculations of the spectral absorption slope of SCDM inanimate organic matter in Lake Teletskoye using equation (9)

λ/λ_0 nm	Station number							$\langle S_{CDOM} \rangle \pm SD$ nm^{-1}
	001	002	005	005	021	k1	1s2	
380/443	0.015	0.017	0.016	0.015	0.018	0.018	0.021	0.017 ± 0.002

4. Conclusions

The spectrum of the vertical light attenuation coefficient in seven bands has been restored, the anomalies of which describe regional features in the upper layer of water and are consistent with direct measurements of the water column spectral reflectance coefficient.

It has been demonstrated that in the case of synchronous measurements of the PAR profile and horizontal irradiance, it is possible to obtain irradiance in physical units at any horizon in the photosynthesis layer.

The obtained values for the spectral absorption coefficient by colored dissolved organic matter and the maximum wavelength of the spectrum of underwater irradiation in the photosynthesis layer coincided with the previously obtained results by employees of the Institute of Biology of the Southern Seas of RAS.

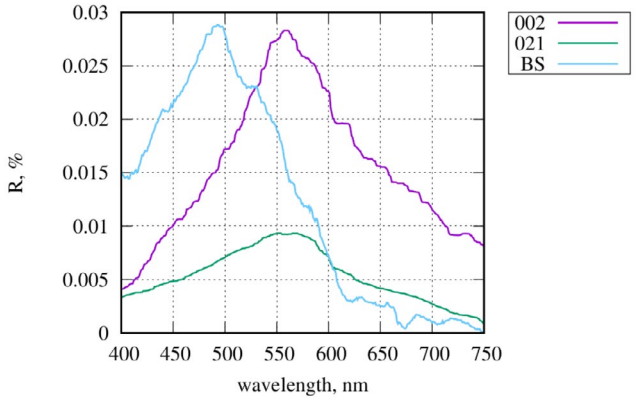

Fig.6. Examples of measurements of the water column spectral reflectance coefficient in Lake Teletskoye in August 2023 at station 002 and 021 and in the deep-water part of the Black Sea in April 2021.

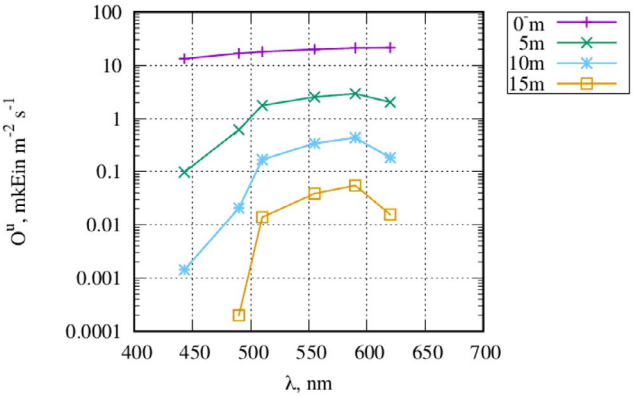

Fig.7. An example of recovery the horizontal irradiance spectrum in physical units for k1 station.

Acknowledgements

The work was carried out within the frameworks of government assignments: for MHI RAS № FNNN-2024-0012, and for IWEP SB RAS №0306-2021-0001 agreements with the administration of the Altai State Nature Reserve. The expeditionary work used scientific equipment of the CSU “Research Vessels of the IWEP SB RAS”.

Conflict of interest

The authors declare no competing interest.

References

Akulova O.B., Bukaty V.I., Sutorikhin I.A. 2017. The influence of natural water components on the spectra of light attenuation coefficient (using the example of reservoirs in the Altai Territory). Optika Atmosfery i Okeana [Atmospheric and Oceanic Optics] 30 (5): 414–419. DOI: 10.15372/AOO20170509 (in Russian)

Akulova O.B., Bukaty V.I., Wagner A.A. et al. 2022. Photosynthetically active solar radiation in Lake Teletskoye during the open water period. Bulletin of the Altai State University 4: 11–17. DOI: 10.14258/izvasu(2022)4-01 (in Russian)

Aslamov I.A., Balin Yu.S., Bashenkhaeva M.V. et al. 2020. Expeditionary works of the LIN SB RAS on Lake Baikal in 2019. Results of expeditionary research in 2019 in the World Ocean, inland waters and on the Spitsbergen archipelago. Conference Proceedings. Sevastopol, pp. 166–171. (in Russian)

Bartlett J.S., Ciotti A.M., Davis R.F. et al. 1998. The spectral effects of clouds on solar irradiance. Journal of Geophysical Research 103 (13): 31,017–31,031. DOI: 10.1029/1998JC900002

Churilova T., Moiseeva N., Efimova T. et al. 2020. Spectral bio-optical properties of lake Baikal (July 2018 and September 2019). Limnology and Freshwater Biology 4: 910–911. DOI: 10.31951/2658-3518-2020-A-4-910

Churilova T.Ya., Moiseeva N.A., Efimova T.V. et al. 2023. Water transparency and spectral downwelling irradiance in the Black and Azov seas and in Lake Teletskoye. Proceedings of SPIE 12780, 29th International Symposium on Atmospheric and Ocean Optics. Atmospheric Physics 1278047. DOI: 10.1117/12.2690845

Hydrobiophysical multiparametric submersible autonomous complex “CONDOR”. 2024. URL: https://dent-s.narod.ru/kondor.html (21.01.2024). (in Russian).

Kopelevich O.V. 1983. Low-parameter models of optical properties of sea water. Ocean Optics. Vol. 1. Physical Optics of the Ocean. Moscow: Nauka, pp. 208-234. (in Russian)

Kopelevich O.V., Burenkov V.I., Ershova S.V. et al. 2004. Application of SeaWiFS data for studying variability of bio-optical characteristics in the Barents, Black and Caspian seas. Deep Sea Research. Part II: Topical Studies in Oceanography 51 (10–11): 1063–1091. DOI: 10.1016/j.dsr2.2003.10.009

Latushkin A.A., Kudinov O.B. 2019. Autonomous sounding meter of photosynthetically active radiation. Materials of the IV All-Russian Scientific Conference of Young Scientists: Comprehensive studies of the World Ocean. Sevastopol: Publishing house MHI RAS, pp. 365–366. (in Russian)

Lee M.E. 2012. Development of hydro-optical instruments at MHI NAS of Ukraine. Environmental Control Systems 17: 7–20. DOI: 10.33075/2220-5861 (in Russian)

Moiseeva N.A., Churilova T.Ya., Efimova T.V. et al. 2023. Spectral bio-optical properties of Lake Teletskoye in summer. Proceedings of SPIE 12780, 29th International Symposium on Atmospheric and Ocean Optics. Atmospheric Physics 1278049. DOI: 10.1117/12.2690958

Selegey V.V., Dehandshutter B., Klerks Ja. et al. 2001. Physical-geographical and geological characteristics of Lake Teletskoye. Proc. Department of Geology and Mineralogy 105: 310. Royal Museum for Central Africa, Tervuren, Belgium, Geol. Sci. Annales.

Shybanov E., Papkova A., Korchemkina E. et al. 2023. Blue color indices as a reference for remote sensing of Black Sea Water. Remote Sensing 15 (14): 3658. DOI: 10.3390/rs15143658

Suetin V.S., Suslin V.V., Korolev S.N. et al. 2002. Assessment of variability of optical properties of water in the Black Sea in summer 1998 based on data from the SEAWIFS satellite instrument. Marine Hydrophysical Journal 6: 44–54. (in Russian)

Suslin V.V., Churilova T.Ya., Latushkin A.A. et al. 2020. Photosynthetically available radiation at the bottom of the northwestern shelf of the Black sea based on regional models and satellite ocean color products and its interannual variability. Fundamental and Applied Hydrophysics 13 (3): 68–77. DOI: 10.7868/S2073667320030053

Sutorikhin I.A., Kolomeitsev A.A., Litvinenko S.A. 2020. Hydrooptical parameters of Lake Teletskoye water during the period of stable summer and winter temperature stratification. Fundamental and Applied Hydrophysics 13 (2): 35–42. DOI: 10.7868/S2073667320020045 (in Russian)